BIOMOLECULES & THERAPEUTICS

Original Article
Biomol Ther 30(4), 368-379 (2022)

High Levels of Hyaluronic Acid Synthase-2 Mediate NRF2-Driven Chemoresistance in Breast Cancer Cells

Bo-Hyun Choi[1], Ingeun Ryoo[2], Kyeong Hwa Sim[1], Hyeon-jin Ahn[1], Youn Ju Lee[1] and Mi-Kyoung Kwak[2,3,*]

[1]Department of Pharmacology, School of Medicine, Daegu Catholic University, Daegu 42472,
[2]Department of Pharmacology and Integrated Research Institute for Pharmaceutical Sciences, The Catholic University of Korea, Bucheon 14662,
[3]College of Pharmacy, The Catholic University of Korea, Bucheon 14662, Republic of Korea

Abstract

Hyaluronic acid (HA), a ligand of CD44, accumulates in some types of tumors and is responsible for tumor progression. The nuclear factor erythroid 2-like 2 (NRF2) regulates cytoprotective genes and drug transporters, which promotes therapy resistance in tumors. Previously, we showed that high levels of CD44 are associated with NRF2 activation in cancer stem like-cells. Herein, we demonstrate that HA production was increased in doxorubicin-resistant breast cancer MCF7 cells (MCF7-DR) via the upregulation of HA synthase-2 (HAS2). HA incubation increased NRF2, aldo-keto reductase 1C1 (AKR1C1), and multidrug resistance gene 1 (MDR1) levels. Silencing of *HAS2* or *CD44* suppressed NRF2 signaling in MCF7-DR, which was accompanied by increased doxorubicin sensitivity. The treatment with a HAS2 inhibitor, 4-methylumbelliferone (4-MU), decreased NRF2, AKR1C1, and MDR1 levels in MCF7-DR. Subsequently, 4-MU treatment inhibited sphere formation and doxorubicin resistance in MCF7-DR. The Cancer Genome Atlas (TCGA) data analysis across 32 types of tumors indicates the amplification of *HAS2* gene is a common genetic alteration and is negatively correlated with the overall survival rate. In addition, high HAS2 mRNA levels are associated with increased NRF2 signaling and poor clinical outcome in breast cancer patients. Collectively, these indicate that HAS2 elevation contributes to chemoresistance and sphere formation capacity of drug-resistant MCF7 cells by activating CD44/NRF2 signaling, suggesting a potential benefit of HAS2 inhibition.

Key Words: HA synthase-2, CD44, Doxorubicin resistance, NRF2, Tumor microenvironment, 4-MU

INTRODUCTION

The tumor microenvironment has been implicated in tumor progression and therapeutic resistance (Kharaishvili *et al*., 2014; Sun, 2016). Hyaluronic acid (HA) is a major component of the extracellular matrix (ECM) in the tumor microenvironment. In solid tumors, HA is responsible for tumor initiation, progression, and tumor resistance (Marozzi *et al*., 2021). HA levels are elevated in malignant tumors, such as colon, ovarian, and breast cancers, and HA accumulation is strongly associated with poor clinical prognosis (Knudson, 1996; Ropponen *et al*., 1998; Anttila *et al*., 2000; Auvinen *et al*., 2000). Mammalian HA is synthesized by three distinct hyaluronic acid synthases (HAS1, HAS2, and HAS3), which produce HA polymers with different molecular masses (Weigel *et al*., 1997; Itano *et al*., 1999). Among the three isoforms, the role of HAS2 in HA synthesis has been well characterized. Due to the lack of HA synthesis, HAS2-*null* mice show severe cardiac and vascular abnormalities, and exhibits a failure in the normal transformation of cardiac endothelial cells into the mesenchyme (Camenisch *et al*., 2000). In tumor cells, HAS2 has been identified to play a role in the invasion and metastasis of tumor cells (Bernert *et al*., 2011; Preca *et al*., 2017; Sheng *et al*., 2021). Clinically, increased HAS2 expression correlates with poor prognosis in several cancers, including pancreatic cancer, breast cancer, and melanoma (Auvinen *et al*., 2014; Poukka *et al*., 2016; Tiainen *et al*., 2016; Yu *et al*., 2021). Therefore, loss of the *HAS2* gene or treatment with 4-methylumbelliferone (4-MU), a small molecule inhibitor of HA synthesis, reduces cancer cell growth and inhibits the malignant phenotype (Li *et al*., 2007; Lokeshwar *et al*., 2010; Okuda *et al*., 2012).

Open Access **https://doi.org/10.4062/biomolther.2022.074**

Received May 30, 2022 **Revised** Jun 2, 2022 **Accepted** Jun 2, 2022
Published Online Jul 1, 2022

***Corresponding Author**
E-mail: mkwak@catholic.ac.kr
Tel: +82-2-2164-6532, Fax: +82-2-2164-4059

The transmembrane molecule, cluster of differentiation 44 (CD44), senses tumor microenvironmental changes by binding to ECM components, such as HA, and transduces extracellular signals to regulate tumor progression. For example, HA-activated CD44 signaling was observed to provoke tumor progression by inducing oncogenic events, including RhoGTPase and matrix metalloproteinase (MMP) signaling (Yu and Stamenkovic, 1999; Bourguignon, 2008; Orgaz *et al*., 2014). Elevated expression levels of HAS2 and CD44 have been detected in aggressive breast cancer cells (Udabage *et al*., 2005). Perturbation of HA-CD44-binding inhibits anchorage-independent growth and metastasis in several cancer cells (Bartolazzi *et al*., 1994; Peterson *et al*., 2000; Ahrens *et al*., 2001; Ghatak *et al*., 2002). Furthermore, the HA-CD44 complex promotes multidrug resistance through the expression of drug efflux transporters. Cross-linking of HA with CD44 induces the nuclear complex formation of NANOG and signal transducer and activator of transcription protein-3 (STAT-3), and this complex activates the expression of multidrug resistance gene 1 (MDR1) in breast cancer cells (Bourguignon *et al*., 2008). In lung cancer cells, CD44 overexpression increases the level of multidrug resistance-associated protein 2 (MRP2) on HA-coated culture plates and induces anticancer drug resistance (Ohashi *et al*., 2007).

Nuclear factor erythroid 2-like 2 (NFE2L2; NRF2) is a key transcription factor that protects cells against oxidative stress by enhancing cytoprotective genes harboring antioxidant response elements (AREs) on their promoters. Under oxidative/electrophilic stress, NRF2 is sequestered from the Kelch-like ECH-associated protein (KEAP1), and transported to the nucleus, where it regulates the expression of phase 2 detoxifying enzymes (e.g., aldo-keto reductase 1C1 [AKR1C1], NAD(P)H quinone oxidoreductase-1 [NQO1]), antioxidant proteins (e.g., glutamate-cysteine ligase modulatory subunit [GCLM]), and drug efflux transporters (e.g., MDR1, breast cancer resistance protein [BCRP]) (Cho and Kleeberger, 2020; Otsuki and Yamamoto, 2020). During the last decade, accumulating evidence has indicated that aberrant activation of NRF2 facilitates tumor growth and survival by inducing cytoprotective genes in cancer cells (Shibata *et al*., 2008; Wang *et al*., 2008; Choi *et al*., 2021a). Similarly, our previous studies showed that silencing of *NRF2* gene in cancer cells reduced the tumor growth and resistance to anticancer drug treatment (Kim *et al*., 2011; Choi *et al*., 2014).

Recently, our findings revealed an association between CD44/NRF2 and cancer stem cell (CSC)-like properties of breast cancer cells (Ryoo *et al*., 2018). The $CD44^{high}$ breast CSC-enriched system showed that CD44-mediated NRF2 activation contributed to the development of CSC-like properties, such as sphere-forming capacity and resistance to anticancer drugs and oxidative stress. However, the involvement of microenvironmental factors, such as HA, in the CD44/NRF2 axis is not yet fully understood. In the current study, we investigated the linkage between HA and CD44/NRF2-induced chemoresistance using doxorubicin-resistant breast and gastric cancer cells and investigated the potential benefit of HAS inhibition for the control of chemoresistance of $NRF2^{high}$ cancer cells.

MATERIALS AND METHODS

Materials

Doxorubicin, 3-(4,5-dimethylthiazol-2-yl)-2,5-diphenyltetrazolium bromide (MTT), 3-(4,5-dimethylthiazol-2-yl)-5-(3-carboxymethoxyphenyl)-2-(4-sulfophenyl)-2H-tetrazolium (MTS), geneticin, hyaluronic acid sodium salt with extra-low molecular weight (8,000-15,000 Da), 4-MU, Mission Lentiviral Packaging mix, and hexadimethrine bromide were purchased from Sigma-Aldrich (Saint Louis, MO, USA). Fluorescein isothiocyanate (FITC)-conjugated CD44 antibody was purchased from BioLegend (San Diego, CA, USA). Additionally, 6-Carboxy-2',7'-dichlorodihydrofluorescein diacetate (carboxy-H_2DCFDA) was purchased from Life Technologies (Carlsbad, CA, USA). Antibodies recognizing NRF2 and glyceraldehyde 3-phosphate dehydrogenase (GAPDH) were obtained from Santa Cruz Biotechnology (Santa Cruz, CA, USA). Antibodies against MDR1 and CD44 were from Cell Signaling Technology (Danvers, MA, USA). Anti-AKR1C1 was purchased from Abnova (Walnut, CA, USA), and anti-HAS-2 antibody was purchased from Abcam (Cambridge, MA, USA). The SYBR premix ExTaq system was obtained from Takara Bio Inc. (Otsu, Japan). The fluorescent dye Hoechst 33342 was obtained from Thermo Fisher Scientific Inc. (Waltham, MA, USA).

Cell culture

The human breast cancer cell line MCF7 was obtained from the American Type Culture Collection (Rockville, MD, USA). Doxorubicin-resistant MCF7-DR cell lines were gifted by Dr. Keon Wook Kang (Seoul National University, Seoul, Korea). SNU620 and SNU620-DR cell lines were purchased from the Korean Cell Line Bank (Seoul, Korea). MCF7/MCF7-DR cells were maintained in Dulbecco's modified Eagle's medium (DMEM), and SNU620/SNU620-DR cells were maintained in Roswell Park Memorial Institute (RPMI) 1640 medium. Both media were supplemented with 10% fetal bovine serum (FBS; Hyclone, Logan, UT, USA) and penicillin/streptomycin (WelGene Inc., Daegu, Korea). The cells were maintained at 37°C in an atmosphere of 5% carbon dioxide (CO_2).

HAS2 overexpression

The HAS2 cDNA open reading frame (ORF) clone (cat. RG224227), and empty control pCMV6-AC-GFP vector (catalog number: PS100010) were purchased from OriGene (Rockville, MD, USA). Lentiviral particles were produced in HEK293T cells following transfection with HAS2-subcloned pCMV6-AC-GFP (HAS2-ov) or the empty vector, and a lentiviral packaging kit (Sigma-Aldrich), as described by the manufacturer. MCF7-DR cells were infected with lentiviral particles in the presence of 8 μg/mL hexadimethrine bromide. Transduction was continued for 48 h, followed by 24 h recovery in complete medium. For the selection of stable transgene-expressing cells, geneticin (G418, 500 μg/mL) was incubated for up to 1 month.

Real-time reverse transcription-polymerase chain reaction (RT-PCR)

Total RNA was extracted from the seeded cells using TRIzol reagent (Thermo Fisher Scientific Inc.). For cDNA synthesis, RT reactions were performed by incubating 200 ng of the total RNA with a reaction mixture, which contained 0.5 μg/μL oligo dT12-18 and 200 U/μL Moloney murine leukemia virus

RT (Life Technologies). Real-time PCR was performed using a Roche Light Cycler (Mannheim, Germany) with the Takara SYBR Premix ExTaq System (Takara Bio Inc.) (Ryu *et al*., 2020). Primers were synthesized by the Bioneer Corporation (Daejeon, Korea), and the primer sequences for the human NRF2, AKR1C1, CD44, MDR1, HAS1-3 and hypoxanthine phosphoribosyltransferase-1 (HPRT1) are as follows: *NRF2*, 5'-ATAGCTGAGCCCAGTATC-3' and 5'-CATGCACGTGAGTGCTCT-3'; *AKR1C1*, 5'-CGAGAAGAACCATGGGTGGA-3' and 5'-GGCCACAAAGGACTGGGTCC-3'; *CD44*, 5'- CGGACACCATGGACAAGTTT-3' and 5'- GAAAGCCTTGCAGAGGTCAG-3'; *MDR1*, 5'-CTATGCTGGATGTTTCCGGT-3' and 5'-TCTTCACCTGGCTCAGT'-3'; *HAS1*, 5'-TACTTTTGGGGATGACCGGC-3' and 5'-AAGTACGACTTGGACCAGCG-3'; *HAS2*, 5'-CCATGGTTGGAGGTGTTGGG-3' and 5'-CTGTACATTCCCAGAGGTCCAC-3'; *HAS3*, 5'-GCGATTCGGTGGACTACATC-3' and 5'-CGTACTTGTTGAGGATCTGGAC-3'; *HPRT1*, 5'-TGGCGTCGTGATTAGTGATG-3' and 5'-GCTACAATGTGATGGCCTCC-3'.

HA measurement

Cells (5×10^5) were incubated in media without serum for 48 h. Then, the supernatant was collected for enzyme-linked immunosorbent assay (ELISA) analysis and particulates were removed by centrifugation. Plasma HA levels were determined by ELISA using a Quantikine Hyaluronan Immunoassay Kit (cat. DHYAL0; R&D Systems, Abingdon, UK), according to the manufacturer's protocol. Optical density values were determined using SPECTRO Star^{Nano} (BMG LABTECH GmbH, Allmendgruen, Ortenberg, Germany) to read the absorbance at 450 and 570 nm.

Western blotting

Cells were lysed with radioimmunoprecipitation assay (RIPA) lysis buffer (50 mM Tris [pH 7.4], 150 mM sodium chloride (NaCl), 1 mM ethylenediaminetetraacetic acid (EDTA), and 1% nonidet P-40 [NP-40]) containing a protease inhibitor cocktail (Sigma-Aldrich). The protein concentration was determined using a bicinchoninic acid assay (BCA) kit (Thermo Scientific, Middletown, VA, USA). The protein samples were separated by electrophoresis on 6-12% sodium dodecyl sulfate (SDS)-polyacrylamide gels and transferred to nitrocellulose membranes (Whatman GmbH, Dassel, Germany) using a Trans-Blot Semi-Dry Cell (Bio-Rad). The membrane was blocked with 3% bovine serum albumin (BSA) for 1 h and incubated with the antibodies. Following the addition of the enhanced chemiluminescence reagent (Thermo Scientific), images were acquired using a GE Healthcare LAS-4000 mini imager (GE Healthcare Sciences, Piscataway, NJ, USA).

MTT/MTS assay

Cells were seeded at a density of 5×10^3 cells/well in 96-well plates. After 24 h of incubation, the cells were treated with doxorubicin, with or without 4-MU. Then, 2 mg/mL of MTT solution (for MCF7/MCF7-DR cells) or 20 μL of MTS reagent (for SNU620/SNU620-DR cells) was added to each well, and cells were incubated for an additional 3 h. MTT reagent was removed after incubation and 100 μL of dimethyl sulfoxide was added to each well (Lee *et al*., 2020; Choi *et al*., 2021b). The absorbance was measured at 540 nm (MTT assay) or 490 nm (MTS assay) using SPECTRO Star^{Nano} (BMG LABTECH GmbH).

siRNA transfection

Predesigned siRNAs for *HAS2*, *NRF2*, *CD44* and a scrambled control were obtained from Bioneer Corporation. Cells were seeded in 6-well plates and transfected with siHAS2, siNRF2, siCD44 or siCTRL using Lipofectamine 2000 reagent (Life Technologies). The next day, the reagent-containing media were removed and cells were recovered with fresh medium.

Immunocytochemical analysis

Cells were plated at a density of 5×10^3 cells/well on cover glass slides. The cells were washed with cold phosphate-buffered saline (PBS) three times and fixed in cold methanol for 10 min. Then, anti-HAS2 antibody (1:200) was incubated in fixed cells at 4°C overnight. The next day, cells were washed with PBS and incubated with Alexa Fluor 488 conjugate-DAM IgG anti-mouse antibody (1:500) at room temperature for 1 h. For nuclear staining, incubation with Hoechst 33342 was performed for 10 min. Fluorescence images were obtained using LSM 710 confocal microscope (Carl Zeiss, Jena, Germany) (Jung *et al*., 2017).

Flow cytometry

Cells were detached using 0.05% trypsin-ethylenediaminetetraacetic acid (EDTA) solution and resuspended in cold PBS containing 2% FBS. Cells were stained with FITC-conjugated CD44 antibody for 30 min. After washing with PBS, cells were analyzed using a Becton-Dickinson FACSCanto (Becton-Dickinson, Milan, Italy) or CytoFLEX (Beckman-Coulter, CA, USA) as described previously (Ryoo *et al*., 2018). Data analysis was performed using FACSDiva (Becton-Dickinson) or CytExpert software (Beckman-Coulter), respectively.

Reactive oxygen species (ROS) measurement

Cellular ROS levels were determined using fluorescent carboxy-H_2DCFDA, as described previously (Ryoo *et al*., 2018). Briefly, the cells were incubated with 30 μM carboxy-H2DCFDA for 30 min, and fluorescence intensity was measured using a 488 nm laser source in a Becton-Dickinson FACSCanto. Data were analyzed using the FACSDiva (Becton-Dickinson).

Sphere culture

Cells were seeded at a density of 2×10^4 cells/mL in 96-well ultralow attachment plates (Corning Costar Corp., Cambridge, MA, USA) and grown in a serum-free DMEM and Nutrient Mixture F-12 medium supplemented with B27 (1:50, Life Technologies), 20 ng/mL epithelial growth factor (EGF), 20 ng/mL basic fibroblast growth factor (R&D System, Minneapolis, MN, USA), 5 μg/mL bovine insulin (Cell Application Inc., San Diego, CA, USA), 0.5 μg/mL hydrocortisone (Sigma-Aldrich), and penicillin/streptomycin (HyClone) as described previously (Ryoo *et al*., 2018). Cells were grown for 3 d for sphere formation, and spheroids were detected using a Carl Zeiss Primovert Microscope (Carl Zeiss).

cBioPortal analysis for the correlation between HAS2 and NRF2 in the cancer genome

To evaluate the *HAS2* gene alteration rates in 32 types of tumors, we downloaded The Cancer Genome Atlas (TCGA) Pan-Cancer Atlas data: Adrenocortical Carcinoma (n=92), Cholangiocarcinoma (n=36), Bladder Urothelial Carcinoma (n=411), Colorectal Adenocarcinoma (n=594), Breast Invasive

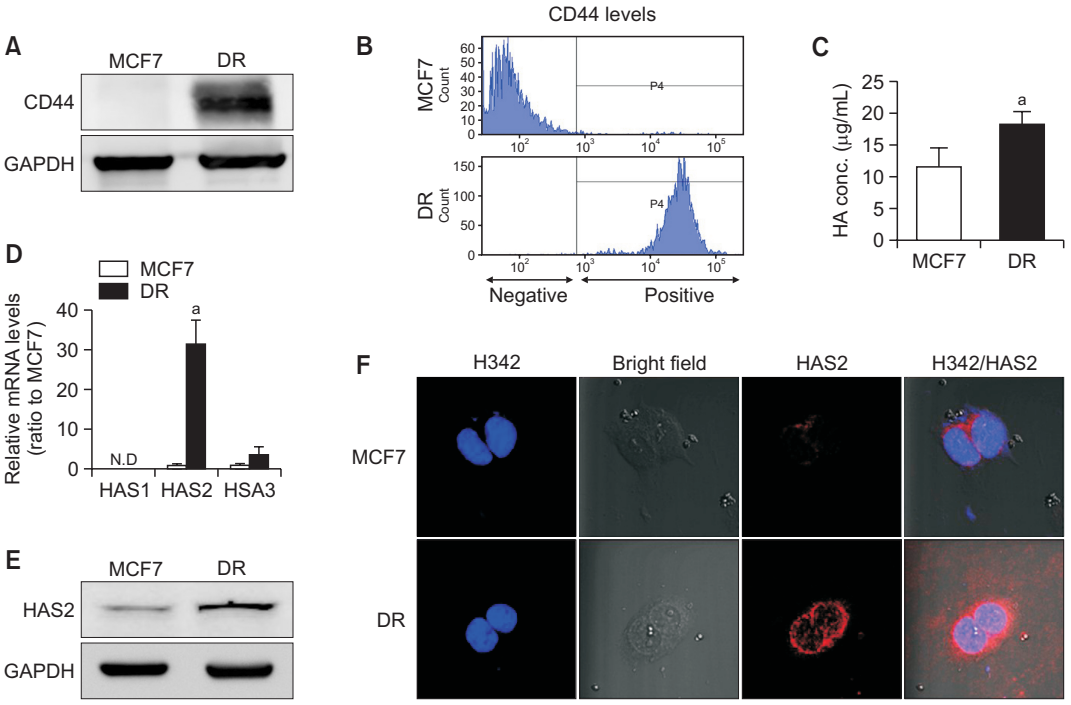

Fig. 1. Doxorubicin-resistant breast cancer MCF7 (MCF7-DR) cells show high levels of hyaluronic acid (HA) through increased expression of HA synthase (HAS)-2. (A) Cluster of differentiation (CD)-44 protein levels were determined in MCF7 and MCF7-DR (DR) cells by western blotting analysis. (B) CD44 expression levels were determined in MCF7 and DR cells using flow cytometry analysis. (C) HA concentration was measured in MCF7 and DR cells by enzyme-linked immunosorbent assay (ELISA) assay. Values represent the mean ± standard deviation (SD) from four experiments. [a]$p<0.05$ compared with MCF7 cells. (D) *HAS1*, *HAS2*, and *HAS3* transcript levels were monitored in MCF7 and DR cells using real-time polymerase chain reaction (qPCR). Values represent the mean ± SD from three experiments. [a]$p<0.05$ compared with MCF7 cells. N.D, not determined. (E) HAS2 protein levels were assessed in MCF7 and DR cells using western blotting analysis. (F) Immunocytochemistry analysis using HAS2 antibody was performed in MCF7 and DR cells. In the case of western blotting results, similar blots were obtained in at least three experiments.

Carcinoma (n=1,084), Brain Lower Grade Glioma (n=514), Glioblastoma Multiforme (n=592), Cervical Squamous Cell Carcinoma (n=297), Esophageal Adenocarcinoma (n=182), Stomach Adenocarcinoma (n=440), Uveal Melanoma (n=80), Head and Neck Squamous Cell Carcinoma (n=523), Kidney Renal Clear Cell Carcinoma (n=512), Kidney Chromophobe (n=65), Kidney Renal Papillary Cell Carcinoma (n=283), Liver Hepatocellular Carcinoma (n=372), Lung Adenocarcinoma (n=566), Lung Squamous Cell Carcinoma (n=487), Diffuse Large B-Cell Lymphoma (n=48), Acute Myeloid Leukemia (n=200), Ovarian Serous Cystadenocarcinoma (n=585), Pancreatic Adenocarcinoma (n=184), Mesothelioma (n=87), Prostate Adenocarcinoma (n=494), Skin Cutaneous Melanoma (n=448), Pheochromocytoma and Paraganglioma (n=178), Sarcoma (n=255), Testicular Germ Cell Tumors (n=149), Thymoma (n=123), Thyroid Carcinoma (n=500), Uterine Corpus Endometrial Carcinoma (n=529), and Uterine Carcinosarcoma (n=57). Kaplan-Meier survival estimates were obtained by log-rank nonparametric test in the cBioPortal (http://www.cbioportal.org). Transcript abundance of *ARK1C1* and *GCLM* has been estimated using RNA-Seq by Estimation Maximization (RSEM) algorithm in log2 scale. P-values are derived from Student's t-test, and q-values are generated from Benjamini-Hochberg procedure. Analyzed data were adopted and visualized from cBioportal.

Statistical analysis

Statistical significance was analyzed using Student's t-test or one-way analysis of variance followed by the Student Newman-Keuls test for multiple comparisons using Prism software (GraphPad Prism, La Jolla, CA, USA).

RESULTS

Doxorubicin-resistant MCF7 cells exhibit increased HA synthesis via upregulation of HAS2

MCF7-DR cells demonstrated increased cell viability following a 72 h incubation with doxorubicin (Supplementary Fig. 1). Similar to our previous report (Ryoo *et al*., 2018), we confirmed the elevated CD44 levels in MCF7-DR cells using western blotting (Fig. 1A). Flow cytometric analysis also showed that over 95% of MCF7-DR cells were CD44-positive cells, while >90% of MCF7 cells were CD44-negative (Fig. 1B). HA is a major ligand for CD44; therefore, we compared HA levels in MCF7-DR cells with those in MCF7 cells. The measurement showed that MCF7-DR cells retained higher HA levels than MCF7 cells, in accordance with a higher CD44 levels (Fig. 1C). There are three subtypes of HAS genes encoding mammalian HAS1, HAS2, and HAS3 (Itano *et al*., 1999). To identify which HAS isotype is responsible for the increased levels of HA in MCF7-DR cells, we measured the mRNA lev-

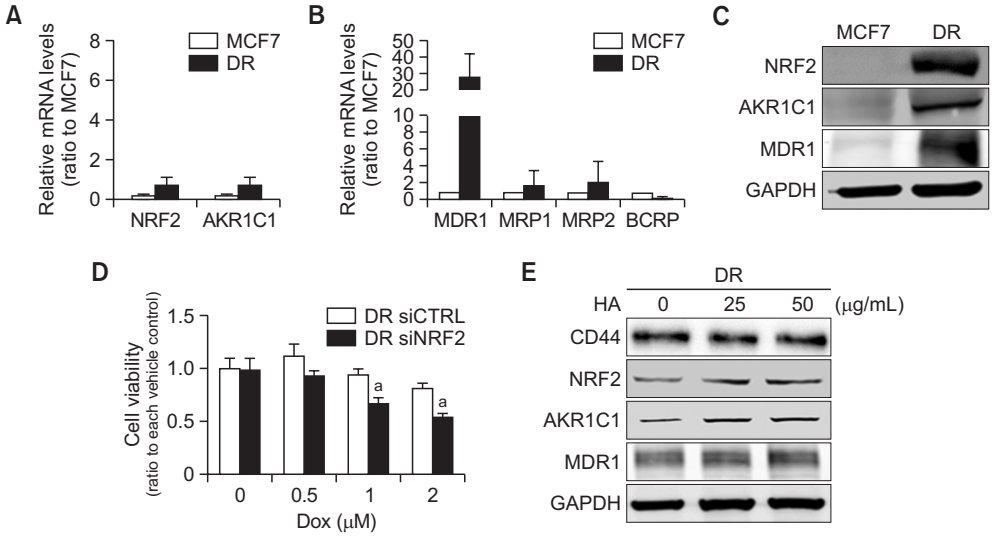

Fig. 2. MCF7-DR cells show activated NRF2 signaling. (A) *NRF2* and aldo-keto reductase 1C1 (*AKR1C1*) transcript levels were monitored in MCF7 and DR cells using relative quantification real-time PCR analysis. Hypoxanthine phosphoribosyltransferase-1 (*HPRT1*) was used as a housekeeping control gene. Data represent ratios with respect to MCF7 and are reported as mean ± SD of three experiments. (B) *MDR1*, *MRP1*, *MRP2*, and *BCRP* transcript levels were monitored in MCF7 and DR cells by relative quantification of real-time PCR analysis. *HPRT1* was used as a housekeeping control gene. Data represent ratios with respect to MCF7 cells and are reported as the mean ± SD of three experiments. (C) NRF2, AKR1C1, and multidrug resistance 1 (MDR1) protein levels were determined using western blotting analysis. (D) Cell viability was monitored after doxorubicin incubation for 72 h in the non-specific control RNA-transfected (siCTRL) or *NRF2*-specific siRNA-transfected (siNRF2) DR cells. Values represent the mean ± SD from four sampled wells. [a]$p<0.05$ compared with the siCTRL. (E) DR cells were treated with HA (25 or 50 μg/mL) for 24 h, and CD44, NRF2, AKR1C1, and MDR1 protein levels were monitored using western blotting analysis. In the case of western blot results, similar blots were obtained in at least three experiments.

els of HAS1-3 by RT-PCR analysis. Among all subtypes of HASs, HAS2 and HAS3 were increased, and HAS2 mRNA levels increased 30-fold in MCF7-DR cells compared to MCF7 cells. HAS1 was rarely expressed in either cell line (Fig. 1D). Western blotting analysis showed that HAS2 protein levels were elevated in MCF7-DR cells (Fig. 1E), and immunocytochemical analysis confirmed the increase in HAS2 levels in MCF7-DR cells (Fig. 1F). Collectively, these results indicate that doxorubicin-resistant MCF7-DR cells exhibit high levels of HA along with elevated CD44, and increased HAS2 expression may be responsible for HA elevation.

HA/CD44 mediates NRF2 activation in MCF7-DR cells

Activated NRF2 signaling contributes to chemoresistance in many types of cancer cells (Choi and Kwak, 2016). Similar to our previous study (Ryoo *et al*., 2018), transcript levels of NRF2 and its target AKR1C1 were elevated by 2- and 6-fold, respectively, in MCF7-DR cells compared to those in MCF7 cells (Fig. 2A). In the measurement of drug efflux transporters, including MDR1, MRP1, MRP2, and BCRP, MDR1 levels were substantially increased in MCF7-DR cells (Fig. 2B). Consistent with these results, MCF7-DR cells exhibited higher levels of NRF2, AKR1C1, and MDR1 proteins in immunoblotting analysis (Fig. 2C). When NRF2 expression was silenced in MCF7-DR cells, doxorubicin sensitivity was significantly enhanced (Fig. 2D), indicating the role of increased NRF2 signaling in the drug resistance of MCF7-DR cells.

Next, to elucidate the effect of HA on NRF2 signaling, we incubated MCF7-DR cells with HA. Immunoblotting analysis revealed that the protein levels of NRF2, AKR1C1, and MDR1 were further increased by HA in a concentration-dependent manner (Fig. 2E). However, there was no significant change in CD44 protein expression after HA treatment. These results suggest that the HA/CD44 axis is involved in NRF2 activation in MCF4-DR cells.

High HAS2 expression is responsible for NRF2 activation and drug resistance in MCF7-DR cells

To investigate the direct role of CD44 on NRF2 signaling, we silenced *CD44* expression in MCF7-DR cells (Fig. 3A). When MCF7-DR cells were transiently transfected with *CD44* siRNA (siCD44), NRF2 levels were diminished, which is similar to the observation made in CSC-enriched breast cancers (Ryoo *et al*., 2018); however, HAS2 levels were not affected by *CD44* silencing (Fig. 3B). Moreover, HA treatment (50 μg/mL) did not show elevations in NRF2 and AKR1C1 in CD44-silenced cells, which indicates HA-induced NRF2 activation is CD44-dependent (Fig. 3C). p62 has been suggested as a noncanonocal NRF2 regulator. High levels of p62 competes with NRF2 for KEAP1 binding, which results in NRF2 liberation and subsequent nuclear accumulation (Komatsu *et al*., 2010; Lau *et al*., 2010). Our previous study has shown that p62 levels were elevated in $CD44^{high}$ CSC-enriched breast cancer cells, and *p62*-silencing could repress NRF2 signaling, which indicates the critical role of p62 in CD44-meidated NRF2 activation (Ryoo *et al*., 2018). In line with this, HA treatment increased p62 levels in the nonspecific RNA-transfected DR cells, whereas, p62 levels were increased in CD44-silenced cells (Fig. 3D). These data indicate that HA-mediated CD44 stimulation led to p62-associated NRF2 activation.

Next, to determine whether increased HAS2 expression is involved in NRF2 activation and doxorubicin resistance in

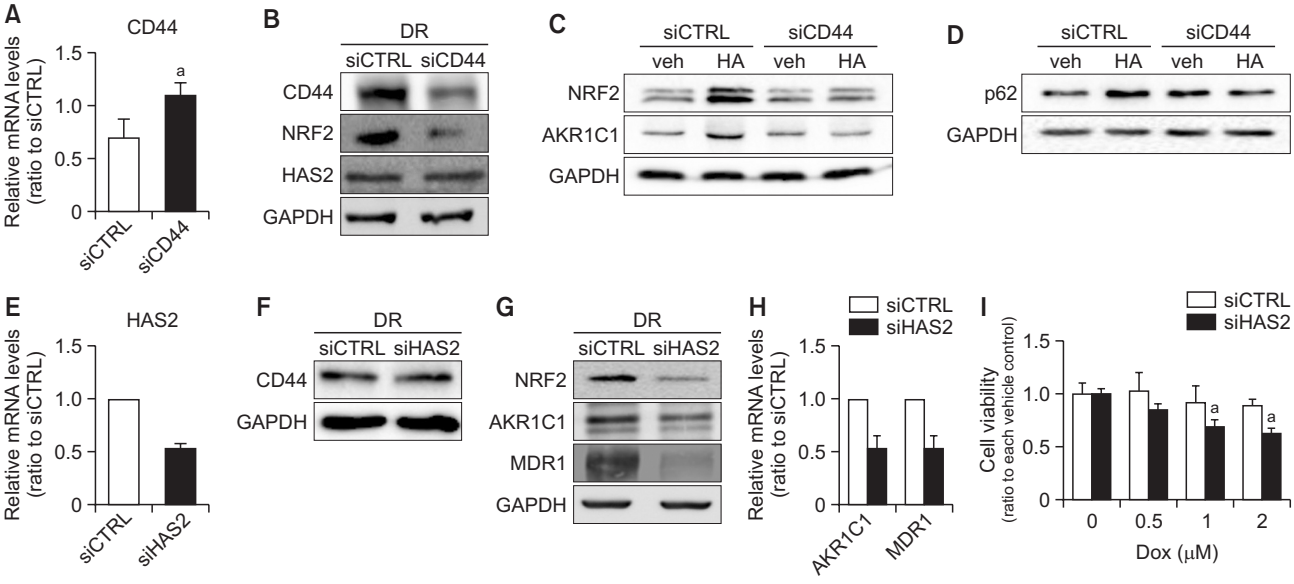

Fig. 3. Inhibition of HAS2 expression sensitizes MCF7-DR cells to doxorubicin via reduction in NRF2 levels. (A) DR cells were transfected with non-specific control RNA (siCTRL) or *CD44*-specific siRNA (siCD44), and *CD44* transcript levels were monitored by relative quantification real-time PCR analysis. *HPRT1* was used as a housekeeping control gene. Data represent ratios with respect to siCTRL. (B) CD44, NRF2, and HAS2 protein levels were determined in siCTRL and CD44-specific siRNA-transfected siCD44 DR cells. (C, D) siCTRL and siCD44 DR cells were incubated with HA (50 ug/mL) for 24 h, and NRF2 and AKR1C1 (C) or p62 (D) levels were measured by western blotting. (E) DR cells were transfected with non-specific control RNA (siCTRL) or *HAS2*-specific siRNA (siHAS2) and *HAS2* transcript levels were monitored by relative quantification real-time PCR analysis. *HPRT1* was used as a housekeeping control gene. Data represent ratios with respect to siCTRL and are reported as the mean ± SD of two experiments. (F) CD44 protein levels were determined in siCTRL and siHAS2 DR cells using western blotting analysis. (G) NRF2, AKR1C1, and MDR1 protein levels were determined in siCTRL and siHAS2 DR cells. (H) *AKR1C1* and *MDR1* transcript levels were monitored in siCTRL and siHAS2 DR cells by relative quantification real-time PCR analysis. *HPRT1* was used as a housekeeping control gene. Data represent ratios with respect to siCTRL and are reported as the mean ± SD of three experiments. (I) Cell viability was monitored after doxorubicin incubation for 72 h in siCTRL and siHAS2 DR cells using 3-(4,5-dimethylthiazol-2-yl)-2,5-diphenyltetrazolium bromide (MTT) assay. Values represent the mean ± SD from four sampled wells. [a]$p<0.05$ compared with siCTRL. In the case of western blot results, similar blots were obtained in at least three experiments.

MCF7-DR cells, HAS2 expression was silenced in MCF7-DR cells (Fig. 3E). Immunoblotting analysis showed that CD44 expression was not affected by *HAS2*-silencing (Fig. 3F). Notably, levels of NRF2, AKR1C1, and MDR1 were all reduced following a loss of HAS2 (Fig. 3G, 3H), which implies a critical role of HAS2 in the NRF2-mediated cancer phenotype. Indeed, cell viability following a 72 h incubation with doxorubicin was repressed in *HAS2*-silenced MCF7-DR cells compared to the non-specific siRNA-transfected cells (Fig. 3I). These data suggest that elevated HAS2 levels are responsible for NRF2 activation and subsequent doxorubicin resistance in MCF7-DR cells.

Pharmacological inhibition of HAS2 leads to the sensitization of MCF7-DR cells to doxorubicin

Next, to confirm the role of HAS2 in NRF2 activation and doxorubicin resistance in MCF7-DR cells, we applied 4-MU, a pharmacological inhibitor of HAS2. When MCF7-DR cells were treated with 4-MU (0.5 mM) for 24 h, HAS2 protein levels were significantly decreased (Fig. 4A). In line with this, the protein levels of NRF2, AKR1C1, and MDR1 were reduced in 4-MU-treated MCF7-DR cells (Fig. 4B). As a result of decreased NRF2 target gene expression, cellular ROS levels were found to be higher in 4-MU-treated MCF7-DR cells than the vehicle-treated MCF7-DR cells (Fig. 4C). As a phenotypic effect, 4-MU treatment suppressed the sphere formation capacity of MCF7-DR cells (Fig. 4D). The average diameters of the vehicle-treated and 4-MU- treated MCF7-DR cells were 67 and 32 μm, respectively. Additionally, when MCF7-DR cells were co-incubated with 4-MU and doxorubicin (2 μM) for 24 h, doxorubicin-induced cytotoxicity was significantly enhanced compared to the doxorubicin-treated group (Fig. 4E). These results show that the pharmacological inhibition of HAS2 could render drug-resistant cancer cells more susceptible to doxorubicin treatment via the inhibition of NRF2 signaling.

HAS2 overexpression mediates NRF2 activation in MCF7-DR cells

Considering the relationship between HAS2 and doxorubicin resistance, we attempted to elucidate the effect of HAS2 overexpression. Forced expression of HAS2 in MCF7-DR cells (HAS2-ov) resulted in increased HAS2 mRNA levels and HA concentration (Fig. 5A, 5B), and led to the increase in NRF2, AKR1C1, and MDR1 levels, without altering CD44 levels (Fig. 5C), thereby confirming the relationship between HAS2 expression and NRF2 activation.

Whether $HAS2^{high}$ cells affect neighboring cancer cells for the enhanced aggressive phenotype is still unknown. As we observed that a significant amount of HA was synthesized by HAS2 in HAS2-overexpressed cells (HAS2-ov), we cultured MCF7-DR cells using HA-enriched medium (conditioned medium from HAS2-ov culture) and the effect on NRF2 and drug

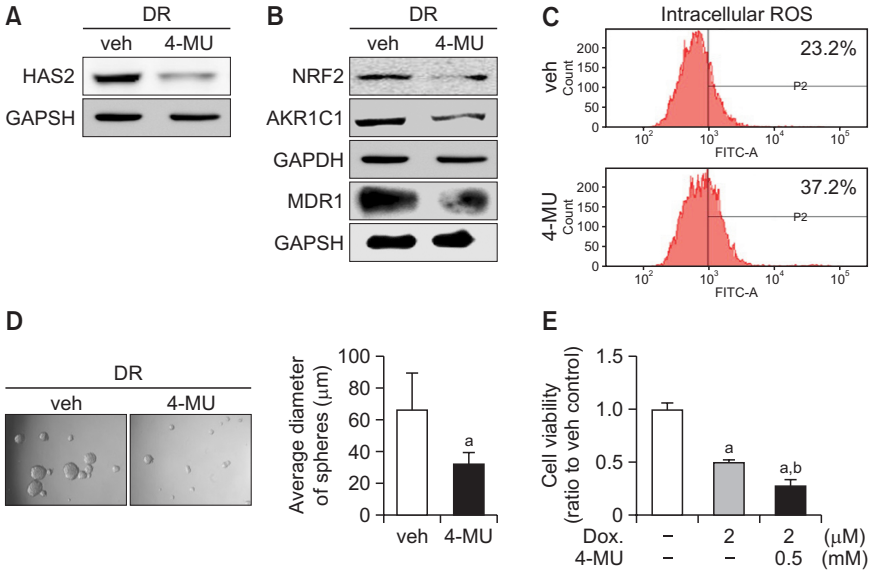

Fig. 4. 4-methylumbelliferone (4-MU) treatment attenuates doxorubicin resistance of MCF7-DR cells. (A) DR cells were incubated with 0.5 mM 4-MU or vehicle (veh) for 24 h. HAS2 protein levels were monitored using western blotting. (B) NRF2, AKR1C1, and MDR1 protein levels were monitored following the treatment of DR cells with 4-MU for 24 h. (C) DR cells were incubated with 4-MU for 24 h, and intracellular ROS levels were determined following the incubation with 6-Carboxy-2',7'-dichlorodihydrofluorescein diacetate (carboxy-H2DCFDA) and subsequent flow cytometry analysis. (D) Sphere formation was assessed after 3 d of sphere culture. Average diameter of spheres was determined using image processing ToupView software (ToupTek Photonics, Zhejiang, China). Values represent the mean ± SD from five different single cells. [a]$p<0.05$ compared with vehicle (veh) treatment. (E) Cell viability was monitored after doxorubicin and 4-MU incubation in DR cells using MTT assay. Values represent the mean ± SD from four sampled wells. [a]$p<0.05$ compared with the vehicle group. [b]$p<0.05$ compared with doxorubicin only group. In the case of western blot results, similar blots were obtained in at least three experiments.

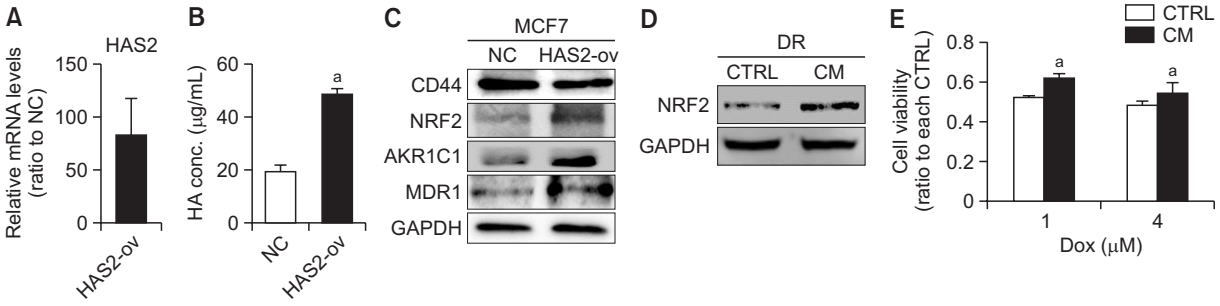

Fig. 5. HAS2 overexpression increased NRF2 signaling. (A) HAS2 was overexpressed in MCF7 (HAS2-ov) cells and relative *HAS2* transcript levels were determined by relative quantification real-time PCR analysis. *HPRT1* was used as a housekeeping control gene. Data represent ratios with respect to negative control (NC) and are reported as the mean ± SD of two experiments. (B) HA concentration was measured in negative control (NC) and HAS2-overexpressing MCF7 (HAS2-ov) cells using ELISA. Values represent the mean ± SD from four sampled wells. [a]$p<0.05$ compared with NC. (C) CD44, NRF2, AKR1C1, and MDR1 protein levels were monitored in NC and HAS2-overexpressing MCF7 (HAS2-ov) cells. (D) Conditioned medium (CM) was harvested from cultured HAS2-ov cells, and then added into MCF7-DR cells and cultured for 24 h. NRF2 protein levels were monitored in the CM-treated or normal medium group (CTRL). (E) Cell viability was monitored after doxorubicin (1 and 4 μM) incubation in CTRL and CM-treated DR cells. Values represent the mean ± SD from 8 sampled wells. [a]$p<0.05$ compared with CTRL. In the case of western blot results, similar blots were obtained in at least three experiments.

sensitivity was monitored. When MCF7-DR cells were incubated with the HA-enriched conditioned medium, the protein levels of NRF2 increased (Fig. 5D), and doxorubicin-induced cytotoxicity was reduced (Fig. 5E). These observations imply the potential interaction of HAS2^{high} cells with neighboring cancer cells for the acquisition of drug resistance through NRF2 activation within the tumor microenvironment.

HAS2 inhibition sensitizes the drug-resistant gastric cancer SNU620-DR cells to doxorubicin

Next, to confirm the relationship between HAS2 and NRF2/chemoresistance, we used additional resistant cancer cell lines. SNU620-DR, a gastric cancer cell line harboring doxorubicin resistance, showed increased cell viability after 72 h of incubation with doxorubicin (Fig. 6A). Compared to the parental cell line, basal protein levels of NRF2, AKR1C1, and CD44 were higher in SNU620-DR cells (Fig. 6B), and flow cytometry

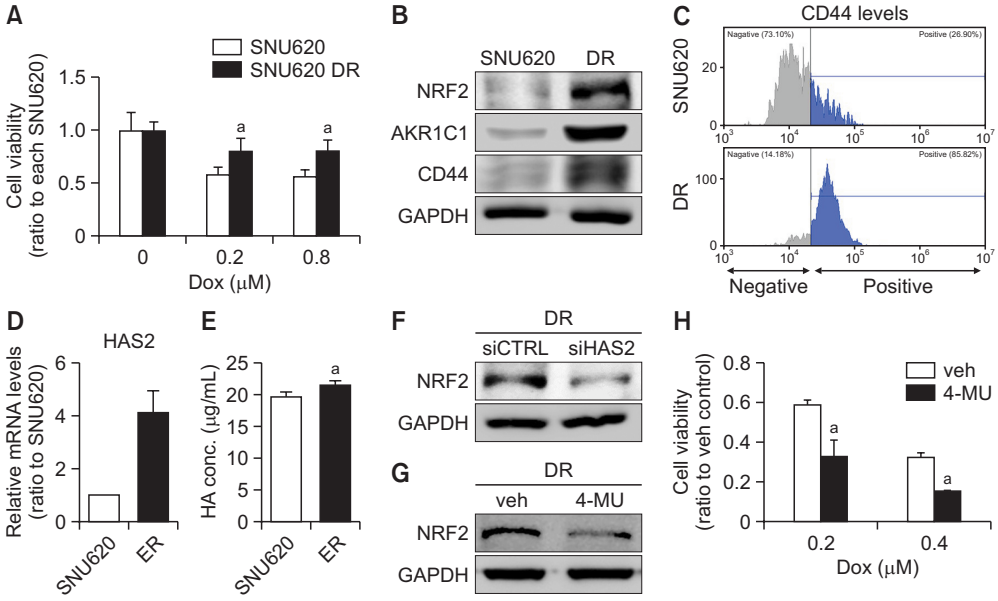

Fig. 6. Increased HAS2 leads to doxorubicin resistance by upregulating NRF2 signaling in gastric cancer SNU620-DR cells. (A) Cell viability was monitored after doxorubicin incubation for 72 h in SNU620 and SNU620-DR cells using 3-(4,5-dimethylthiazol-2-yl)-5-(3-carboxymethoxyphenyl)-2-(4-sulfophenyl)-2H-tetrazolium (MTS) assay. Values represent the mean ± SD from 8 sampled wells. [a]p<0.05 compared with SNU620. (B) NRF2, AKR1C1, and CD44 protein levels were monitored in SNU620 and SNU620-DR (DR) cells using western blotting analysis. (C) CD44 expression levels were determined in SNU620 and DR cells using flow cytometry analysis. (D) *HAS2* transcript levels were determined in SNU620 and SNU620-DR cells by relative quantification real-time PCR analysis. *HPRT1* was used as a housekeeping control gene. Data represent ratios with respect to SNU620 and are reported as the mean ± SD of two experiments. (E) HA concentration was measured in SNU620 and SNU620-DR cells using ELISA. Values represent the mean ± SD of duplicated sample measurements. [a]p<0.05 compared with SNU620. (F) SNU620-DR was transfected with non-specific control RNA (siCTRL) or *HAS2*-specific siRNA (siHAS2), and NRF2 protein levels were monitored. (G) SNU620-DR was incubated with vehicle (veh) or 4-MU (5 mM) for 24 h, and NRF2 protein levels were monitored. (H) Cell viability was monitored after doxorubicin and 4-MU incubation in DR cells using MTS assay. Values represent the mean ± SD of duplicate sample measurements. [a]p<0.05 compared with vehicle (veh) group. In the case of western blot results, similar blots were obtained in at least three experiments.

analysis showed that 85.82% of SNU620 DR cells retained CD44-positive population, while only 26.90 % of SNU620 parental cells were CD44-positive (Fig. 6C). Consistently, HAS2 and HA concentrations were elevated in SNU620-DR cells (Fig. 6D, 6E). Similar to MCF7-DR cells, genetic silencing or pharmacological inhibition of HAS2 decreased NRF2 expression (Fig. 6F, 6G). When SNU620-DR cells were treated with 4-MU for 24 h, these cells showed increased sensitivity to doxorubicin treatment compared to the vehicle-treated group (Fig. 6H). These results confirm that targeting HAS2 might be an effective strategy to overcome the anticancer resistance of NRF2^{high} cancers.

High HAS2 levels are associated with activation of NRF2 signaling and poor clinical outcome in patients with breast cancer

To investigate the clinical importance of HAS2 in tumor patients, we analyzed clinical data using cBioportal platform. TCGA Pan-Cancer Atlas data analysis across 32 types of cancer revealed a higher alteration frequency of *HAS2* genes in several tumors (Supplementary Fig. 2). Among the genetic alteration types (amplification, deep deletion, mutation, structural variant, and multiple alterations), gene amplification is the most frequent alteration type in *HAS2* and, of particular, *HAS2* amplification is relatively common in patients with ovarian epithelial tumor (22.86 % of 398 cases), esophageal squamous cell carcinoma (13.68 % of 95 cases), and invasive breast carcinoma (12.85 % of 996 cases) (Fig. 7A). We assessed the clinical relationship between *HAS2* amplification and overall survival of cancer patients by Kaplan-Meier estimate analysis. It revealed a shorter overall survival rate in patients with amplified HAS2 gene (median survival months=74.73) compared to those with unamplified HAS2 gene (median survival months=88.86) (Fig. 7B).

Next, we specifically analyzed breast TCGA data for patients with breast invasive carcinoma. Among 996 breast cancer patients, 22 patients exhibited higher HAS2 mRNA levels (z-score >=2) compared to the unaltered mRNA group. We additionally found that HAS2-high breast cancer patients showed a shorter overall survival rate (median survival months=91.99) than the unaltered HAS2 gene group (median survival months=130.16) (Fig. 7C). Moreover, HAS2 mRNA levels were associated with increased mRNA levels of AKR1C1 and GCLM in these patients. Mean log2 mRNA expressions of AKR1C1 were 6.34, and 7.32 in the unaltered and HAS2-high group, respectively (Fig. 7D). GCLM mRNA levels were also higher in the HAS2-high patients compared to the unaltered group (Fig. 7E). Collectively, these results demonstrate that HAS2 expression is related to activation of NRF2 signaling, and higher HAS2 levels are associated with poor clinical outcomes in breast cancer patients.

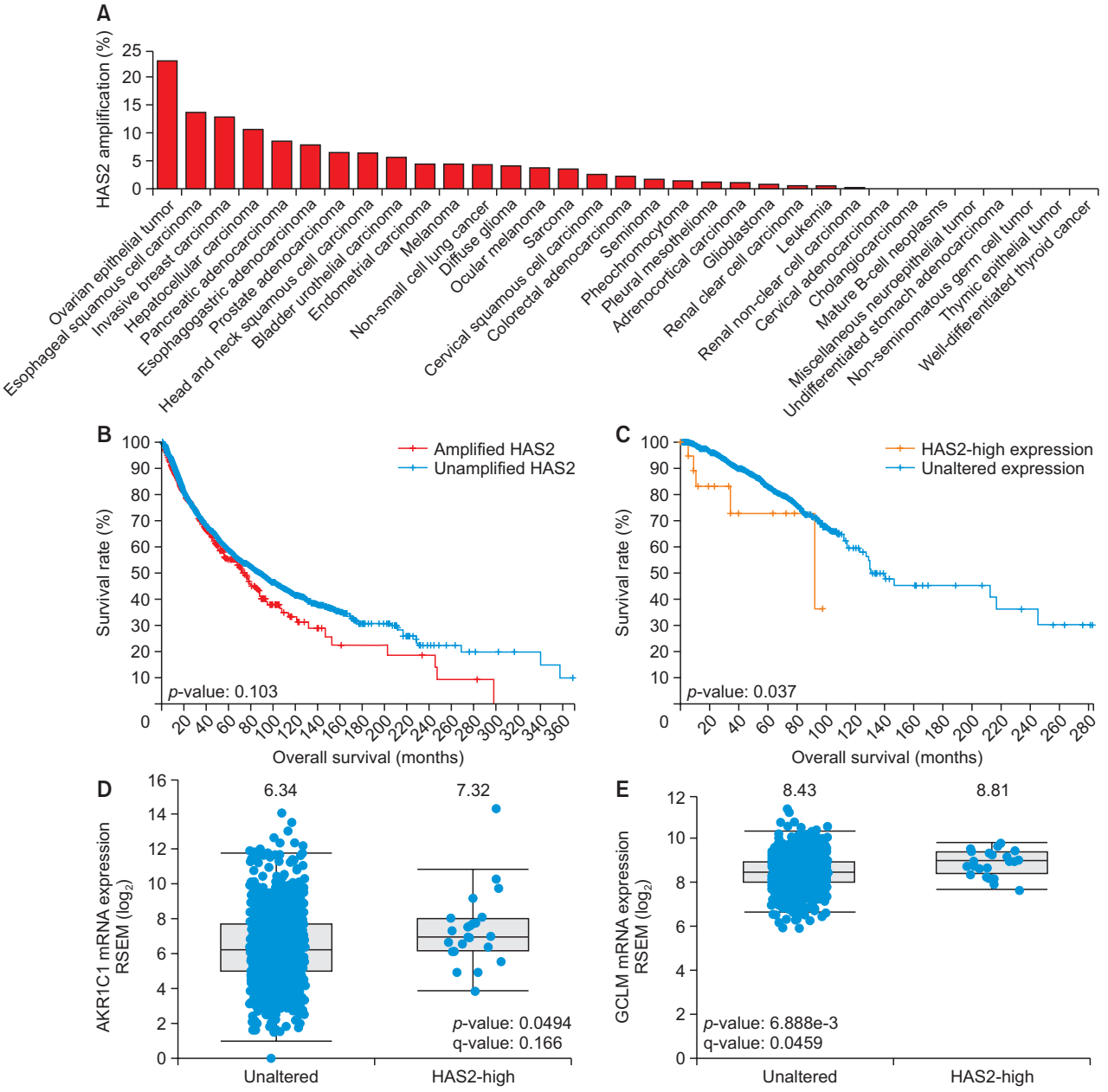

Fig. 7. Association of high HAS2 levels with NRF2 activation and poor clinical outcome in breast cancer patients. (A) HAS2 amplification rate across 32 types of tumor. (B) Overall survival rates of 32 types of tumor patients with amplified *HAS2* (n=554) *vs* unamplified *HAS2* (n=9,262). (C) Overall survival rates of breast cancer patients with high HAS2 mRNA levels (n=22) *vs* unaltered mRNA levels (n=974). (D, E) Correlation of HAS2 mRNA levels (HAS2-high and unaltered) with AKR1C1 (D) and GCLM (E) mRNA levels. Values are shown in (RNA Seq V2 RSEM) in log2 scale. All plots generated by cBioPortal were modified.

DISCUSSION

Despite tremendous advances in anticancer therapeutic strategies, tumor resistance continues to be a principal limiting factor for successful cancer treatment. Recent studies indicate that the tumor microenvironment can be a promising target for overcoming tumor resistance (Son *et al*., 2017; Balaji *et al*., 2021). HA is an important component of the extracellular matrix and is composed of the tumor microenvironment. HA maintains tissue integrity and intracellular activities, such as cell-to-cell adhesion, wound healing, and morphogenesis (Prestwich, 2011). In particular, HA contributes to cancer cell growth, progression, and malignancy in several cancer types. For example, breast cancer cells exhibit high HA levels, which are related to breast cancer growth and progression (Auvinen *et al*., 2013; Bohrer *et al*., 2014). Clinically, high levels of HA secreted from malignant tumors are associated with poor prognosis (Ropponen *et al*., 1998; Anttila *et al*., 2000; Auvinen *et al*., 2000).

CD44 is an important cell surface receptor for HA. Consid-

ering that high levels of HA are detected in the tumor stroma, high CD44 expression contributes to HA-mediated cellular signaling in cancer (Bourguignon *et al*., 2003, 2014). HA/CD44 interaction initiates the Src-ERK signaling cascade, which, in turn, maintains AKT and mTOR activity (Yang *et al*., 2020). HA binding to CD44 in breast tumor cells activates transforming growth factor-β (TGF-β) receptor signaling, which subsequently increases Smad2/3 phosphorylation (Bourguignon *et al*., 2002). Furthermore, it is known that the subpopulation of CD44-positive cells demonstrates CSC phenotypes, such as self-renewal and differentiation capacity. Takaishi *et al*. (2009) reported that all SCID mice implanted with CD44-positive gastric cancer cell fraction could develop tumors in the skin and stomach, whereas CD44-negative cells did not generate tumors. In addition, the CD44-positive subpopulation showed much higher chemo- and radiation-resistance. Notably, this study showed that CD44-positive cells were surrounded by a thick stroma containing numerous immune cells and stromal cells. These results indicate that secreted factors from the tumor microenvironment could mitigate CD44 regulatory signaling and CSC properties (Takaishi *et al*., 2009). The $CD44^{+}/CD24^{-}$ population from ovarian cancer cells exhibited increased differentiation, invasion, and resistance to chemotherapy, which are related to clinical endpoints with a high risk of recurrence and shortened progression-free survival rate (Meng *et al*., 2012). In addition, our previous studies have shown that the $CD44^{high}$ CSC population from breast cancer cells displays anticancer therapy resistance owing to a high NRF2 level, which leads to an increased level of antioxidants and detoxifying enzymes. Accordingly, *NRF2*-knockdown attenuated cancer cell proliferation and chemoresistance in this $CD44^{high}$ subpopulation (Ryoo *et al*., 2018).

Since HAS2 upregulates the expression of mesenchymal markers, such as N-cadherin and vimentin, and the formation of invadopodia, cancer cells expressing a higher level of HAS2 can interact with CD44-positive cancer cells in the tumor microenvironment, which causes these cells to have a more metastatic phenotype (Sheng *et al*., 2021). In the current study, we demonstrated that enhanced HAS2 levels cause HA elevation, thereby activating CD44-mediated NRF2 activation, which promotes tumor resistance in breast cancer cells. Among the three major HASs, HAS2 was markedly upregulated in two types of doxorubicin-resistant cancer cell lines (MCF7-DR and SNU620-DR). The direct interaction between HAS2 levels and tumor resistance was confirmed by the effect of pharmacologic and genetic inhibition or overexpression of HAS2. We showed higher HA levels in drug-resistant cancer cell lines, which correlated with NRF2 activation and subsequent resistance to anticancer treatment. Our results also clarified that 4-MU treatment led to a reduction in NRF2 levels, which subsequently resulted in increased doxorubicin sensitivity. These results reveal a novel interplay between HAS2 and CD44/NRF2 signaling, which correlates with tumor resistance. In accordance with our results, increased HAS2 levels were observed in ovarian cancer cells at recurrence following chemotherapy (Lokman *et al*., 2019). Chemoresistant lymphoma cells also produce higher levels of HA, with greater expression of HAS2 (Qin *et al*., 2011).

Previously, TCGA breast cancer datasets indicated that aberrant amplification of the *HAS2* gene is involved in poor overall survival in patients with breast cancer. Approximately 13 % of breast cancers show *HAS2* amplification, and 25% of metaplastic breast cancers have *HAS2* gene amplification (Chokchaitaweesuk *et al*., 2019). In our analysis, the TCGA dataset of cancer patients across 32 tumor types showed that invasive breast carcinoma was placed 3rd with a high amplification rate of *HAS2* gene followed by ovarian epithelial tumor and esophageal squamous cell carcinoma (Fig. 7A). *HAS2* amplification was positivelt associated with poor clinical outcome in 32 types of tumor patients (Fig. 7B), and this relationship was more evident when analyzing overall survival rate in breast cancer patiemts with high HAS2 mRNA levels (Fig. 7C). Moreover, in these breast cancer patients, there were positive correlation between HAS2 mRNA levels and AKR1C1 as well as GCLM mRNA levels (Fig. 7D), which is in line with our *in vitro* demonstrations of HAS2-meidated NRF2 signaling activation.

It is still not clear how HAS2 is upregulated in drug-resistant cancer cells. Some factors are known to affect HAS2 expression. Estradiol can stimulate HAS2 mRNA expression when combined with insulin-like growth factor-1, insulin, and follicle-stimulating hormone (Chavoshinejad *et al*., 2016). The TGF-β/Smad4 signaling pathway can activate the HAS2-HA system (Li *et al*., 2020). In the mammalian ovary, epigenetic factor microRNA-574 directly inhibits HAS2 expression and subsequently improves oocyte maturation (Pan *et al*., 2018). We demonstrate HAS2 overexpression breast cancer cells activate NRF2 signaling (Fig. 5). Since NRF2 activation by HA was observed and showed resistance to chemotherapy, these results suggest that HA production from cancer-associated fibroblasts (CAFs) can activate NRF2 signaling, which causes tumor resistance. In this case, pharmacological inhibition of NRF2 or HAS2 could be a therapeutic strategy for tumor resistance.

In summary, our results indicate that increased HAS2 levels lead to doxorubicin resistance in breast and gastric cancer cells via the activation of HA/CD44 and NRF2 signaling. These results provide an in-depth understanding of the interaction between tumor microenvironmental HA and NRF2-driven chemoresistance, and further suggest that HAS2 is a novel target to control the therapeutic resistance of NRF2-high cancers.

CONFLICT OF INTEREST

The authors confirm that there are no conflicts of interest.

ACKNOWLEDGMENTS

This work was supported by a National Research Foundation of Korea (NRF) grant funded by the Korean government (MSIT) (2018R1A2A1A05078894, 2017R1A6A3A11030293, and 2021R1C1C1006881).

REFERENCES

Ahrens, T., Sleeman, J. P., Schempp, C. M., Howells, N., Hofmann, M., Ponta, H., Herrlich, P. and Simon, J. C. (2001) Soluble CD44 inhibits melanoma tumor growth by blocking cell surface CD44 binding to hyaluronic acid. *Oncogene* **20**, 3399-3408.

Anttila, M. A., Tammi, R. H., Tammi, M. I., Syrjänen, K. J., Saarikoski, S. V. and Kosma, V. M. (2000) High levels of stromal hyaluronan predict poor disease outcome in epithelial ovarian cancer. *Cancer*

Res. **60**, 150-155.
Auvinen, P., Rilla, K., Tumelius, R., Tammi, M., Sironen, R., Soini, Y., Kosma, V. M., Mannermaa, A., Viikari, J. and Tammi, R. (2014) Hyaluronan synthases (HAS1-3) in stromal and malignant cells correlate with breast cancer grade and predict patient survival. *Breast Cancer Res. Treat.* **143**, 277-286.
Auvinen, P., Tammi, R., Kosma, V. M., Sironen, R., Soini, Y., Mannermaa, A., Tumelius, R., Uljas, E. and Tammi, M. (2013) Increased hyaluronan content and stromal cell CD44 associate with HER2 positivity and poor prognosis in human breast cancer. *Int. J. Cancer* **132**, 531-539.
Auvinen, P., Tammi, R., Parkkinen, J., Tammi, M., Agren, U., Johansson, R., Hirvikoski, P., Eskelinen, M. and Kosma, V. M. (2000) Hyaluronan in peritumoral stroma and malignant cells associates with breast cancer spreading and predicts survival. *Am. J. Pathol.* **156**, 529-536.
Balaji, S., Kim, U., Muthukkaruppan, V. and Vanniarajan, A. (2021) Emerging role of tumor microenvironment derived exosomes in therapeutic resistance and metastasis through epithelial-to-mesenchymal transition. *Life Sci.* **280**, 119750.
Bartolazzi, A., Peach, R., Aruffo, A. and Stamenkovic, I. (1994) Interaction between CD44 and hyaluronate is directly implicated in the regulation of tumor development. *J. Exp. Med.* **180**, 53-66.
Bernert, B., Porsch, H. and Heldin, P. (2011) Hyaluronan synthase 2 (HAS2) promotes breast cancer cell invasion by suppression of tissue metalloproteinase inhibitor 1 (TIMP-1). *J. Biol. Chem.* **286**, 42349-42359.
Bohrer, L. R., Chuntova, P., Bade, L. K., Beadnell, T. C., Leon, R. P., Brady, N. J., Ryu, Y., Goldberg, J. E., Schmechel, S. C., Koopmeiners, J. S., McCarthy, J. B. and Schwertfeger, K. L. (2014) Activation of the FGFR-STAT3 pathway in breast cancer cells induces a hyaluronan-rich microenvironment that licenses tumor formation. *Cancer Res.* **74**, 374-386.
Bourguignon, L. Y. (2008) Hyaluronan-mediated CD44 activation of RhoGTPase signaling and cytoskeleton function promotes tumor progression. *Semin. Cancer Biol.* **18**, 251-259.
Bourguignon, L. Y., Peyrollier, K., Xia, W. and Gilad, E. (2008) Hyaluronan-CD44 interaction activates stem cell marker Nanog, Stat-3-mediated MDR1 gene expression, and ankyrin-regulated multidrug efflux in breast and ovarian tumor cells. *J. Biol. Chem.* **283**, 17635-17651.
Bourguignon, L. Y., Shiina, M. and Li, J. J. (2014) Hyaluronan-CD44 interaction promotes oncogenic signaling, microRNA functions, chemoresistance, and radiation resistance in cancer stem cells leading to tumor progression. *Adv. Cancer Res.* **123**, 255-275.
Bourguignon, L. Y., Singleton, P. A., Zhu, H. and Diedrich, F. (2003) Hyaluronan-mediated CD44 interaction with RhoGEF and Rho kinase promotes Grb2-associated binder-1 phosphorylation and phosphatidylinositol 3-kinase signaling leading to cytokine (macrophage-colony stimulating factor) production and breast tumor progression. *J. Biol. Chem.* **278**, 29420-29434.
Bourguignon, L. Y., Singleton, P. A., Zhu, H. and Zhou, B. (2002) Hyaluronan promotes signaling interaction between CD44 and the transforming growth factor beta receptor I in metastatic breast tumor cells. *J. Biol. Chem.* **277**, 39703-39712.
Camenisch, T. D., Spicer, A. P., Brehm-Gibson, T., Biesterfeldt, J., Augustine, M. L., Calabro, A., Jr., Kubalak, S., Klewer, S. E. and McDonald, J. A. (2000) Disruption of hyaluronan synthase-2 abrogates normal cardiac morphogenesis and hyaluronan-mediated transformation of epithelium to mesenchyme. *J. Clin. Invest.* **106**, 349-360.
Chavoshinejad, R., Marei, W. F., Hartshorne, G. M. and Fouladi-Nashta, A. A. (2016) Localisation and endocrine control of hyaluronan synthase (HAS) 2, HAS3 and CD44 expression in sheep granulosa cells. *Reprod. Fertil. Dev.* **28**, 765-775.
Cho, H. Y. and Kleeberger, S. R. (2020) Mitochondrial biology in airway pathogenesis and the role of NRF2. *Arch. Pharm. Res.* **43**, 297-320.
Choi, B.-H., Kim, J. M. and Kwak, M.-K. (2021a) The multifaceted role of NRF2 in cancer progression and cancer stem cells maintenance. *Arch. Pharm. Res.* **44**, 263-280.
Choi, B.-h. and Kwak, M.-K. (2016) Shadows of NRF2 in cancer: resistance to chemotherapy. *Curr. Opin. Toxicol.* **1**, 20-28.
Choi, B. H., Ryoo, I. G., Kang, H. C. and Kwak, M. K. (2014) The sensitivity of cancer cells to pheophorbide a-based photodynamic therapy is enhanced by Nrf2 silencing. *PLoS ONE* **9**, e107158.
Choi, S. M., Cho, Y. S., Park, G., Lee, S. K. and Chun, K. S. (2021b) Celecoxib induces apoptosis through Akt inhibition in 5-fluorouracil-resistant gastric cancer cells. *Toxicol. Res.* **37**, 25-33.
Chokchaitaweesuk, C., Kobayashi, T., Izumikawa, T. and Itano, N. (2019) Enhanced hexosamine metabolism drives metabolic and signaling networks involving hyaluronan production and O-GlcNAcylation to exacerbate breast cancer. *Cell Death Dis.* **10**, 803.
Ghatak, S., Misra, S. and Toole, B. P. (2002) Hyaluronan oligosaccharides inhibit anchorage-independent growth of tumor cells by suppressing the phosphoinositide 3-kinase/Akt cell survival pathway. *J. Biol. Chem.* **277**, 38013-38020.
Itano, N., Sawai, T., Yoshida, M., Lenas, P., Yamada, Y., Imagawa, M., Shinomura, T., Hamaguchi, M., Yoshida, Y., Ohnuki, Y., Miyauchi, S., Spicer, A. P., McDonald, J. A. and Kimata, K. (1999) Three isoforms of mammalian hyaluronan synthases have distinct enzymatic properties. *J. Biol. Chem.* **274**, 25085-25092.
Jung, K. A., Lee, S. and Kwak, M. K. (2017) NFE2L2/NRF2 activity is linked to mitochondria and AMP-activated protein kinase signaling in cancers through miR-181c/mitochondria-encoded cytochrome c oxidase regulation. *Antioxid. Redox Signal.* **27**, 945-961.
Kharaishvili, G., Simkova, D., Bouchalova, K., Gachechiladze, M., Narsia, N. and Bouchal, J. (2014) The role of cancer-associated fibroblasts, solid stress and other microenvironmental factors in tumor progression and therapy resistance. *Cancer Cell Int.* **14**, 41.
Kim, T. H., Hur, E. G., Kang, S. J., Kim, J. A., Thapa, D., Lee, Y. M., Ku, S. K., Jung, Y. and Kwak, M. K. (2011) NRF2 blockade suppresses colon tumor angiogenesis by inhibiting hypoxia-induced activation of HIF-1α. *Cancer Res.* **71**, 2260-2275.
Knudson, W. (1996) Tumor-associated hyaluronan. Providing an extracellular matrix that facilitates invasion. *Am. J. Pathol.* **148**, 1721-1726.
Komatsu, M., Kurokawa, H., Waguri, S., Taguchi, K., Kobayashi, A., Ichimura, Y., Sou, Y. S., Ueno, I., Sakamoto, A., Tong, K. I., Kim, M., Nishito, Y., Iemura, S., Natsume, T., Ueno, T., Kominami, E., Motohashi, H., Tanaka, K. and Yamamoto, M. (2010) The selective autophagy substrate p62 activates the stress responsive transcription factor Nrf2 through inactivation of Keap1. *Nat. Cell Biol.* **12**, 213-223.
Lau, A., Wang, X. J., Zhao, F., Villeneuve, N. F., Wu, T., Jiang, T., Sun, Z., White, E. and Zhang, D. D. (2010) A noncanonical mechanism of Nrf2 activation by autophagy deficiency: direct interaction between Keap1 and p62. *Mol. Cell. Biol.* **30**, 3275-3285.
Lee, J. K., Lee, H. E., Yang, G., Kim, K. B., Kwack, S. J. and Lee, J. Y. (2020) Para-phenylenediamine, an oxidative hair dye ingredient, increases thymic stromal lymphopoietin and proinflammatory cytokines causing acute dermatitis. *Toxicol. Res.* **36**, 329-336.
Li, X., Du, X., Yao, W., Pan, Z. and Li, Q. (2020) TGF-β/SMAD4 signaling pathway activates the HAS2-HA system to regulate granulosa cell state. *J. Cell. Physiol.* **235**, 2260-2272.
Li, Y., Li, L., Brown, T. J. and Heldin, P. (2007) Silencing of hyaluronan synthase 2 suppresses the malignant phenotype of invasive breast cancer cells. *Int. J. Cancer* **120**, 2557-2567.
Lokeshwar, V. B., Lopez, L. E., Munoz, D., Chi, A., Shirodkar, S. P., Lokeshwar, S. D., Escudero, D. O., Dhir, N. and Altman, N. (2010) Antitumor activity of hyaluronic acid synthesis inhibitor 4-methylumbelliferone in prostate cancer cells. *Cancer Res.* **70**, 2613-2623.
Lokman, N. A., Price, Z. K., Hawkins, E. K., Macpherson, A. M., Oehler, M. K. and Ricciardelli, C. (2019) 4-Methylumbelliferone inhibits cancer stem cell activation and overcomes chemoresistance in ovarian cancer. *Cancers (Basel)* **11**, 1187.
Marozzi, M., Parnigoni, A., Negri, A., Viola, M., Vigetti, D., Passi, A., Karousou, E. and Rizzi, F. (2021) Inflammation, extracellular matrix remodeling, and proteostasis in tumor microenvironment. *Int. J. Mol. Sci.* **22**, 8102.
Meng, E., Long, B., Sullivan, P., McClellan, S., Finan, M. A., Reed, E., Shevde, L. and Rocconi, R. P. (2012) CD44+/CD24- ovarian cancer cells demonstrate cancer stem cell properties and correlate to survival. *Clin. Exp. Metastasis* **29**, 939-948.

Ohashi, R., Takahashi, F., Cui, R., Yoshioka, M., Gu, T., Sasaki, S., Tominaga, S., Nishio, K., Tanabe, K. K. and Takahashi, K. (2007) Interaction between CD44 and hyaluronate induces chemoresistance in non-small cell lung cancer cell. *Cancer Lett.* **252**, 225-234.

Okuda, H., Kobayashi, A., Xia, B., Watabe, M., Pai, S. K., Hirota, S., Xing, F., Liu, W., Pandey, P. R., Fukuda, K., Modur, V., Ghosh, A., Wilber, A. and Watabe, K. (2012) Hyaluronan synthase HAS2 promotes tumor progression in bone by stimulating the interaction of breast cancer stem-like cells with macrophages and stromal cells. *Cancer Res.* **72**, 537-547.

Orgaz, J. L., Pandya, P., Dalmeida, R., Karagiannis, P., Sanchez-Laorden, B., Viros, A., Albrengues, J., Nestle, F. O., Ridley, A. J., Gaggioli, C., Marais, R., Karagiannis, S. N. and Sanz-Moreno, V. (2014) Diverse matrix metalloproteinase functions regulate cancer amoeboid migration. *Nat. Commun.* **5**, 4255.

Otsuki, A. and Yamamoto, M. (2020) Cis-element architecture of Nrf2-sMaf heterodimer binding sites and its relation to diseases. *Arch. Pharm. Res.* **43**, 275-285.

Pan, B., Toms, D. and Li, J. (2018) MicroRNA-574 suppresses oocyte maturation via targeting hyaluronan synthase 2 in porcine cumulus cells. *Am. J. Physiol. Cell Physiol.* **314**, C268-C277.

Peterson, R. M., Yu, Q., Stamenkovic, I. and Toole, B. P. (2000) Perturbation of hyaluronan interactions by soluble CD44 inhibits growth of murine mammary carcinoma cells in ascites. *Am. J. Pathol.* **156**, 2159-2167.

Poukka, M., Bykachev, A., Siiskonen, H., Tyynelä-Korhonen, K., Auvinen, P., Pasonen-Seppänen, S. and Sironen, R. (2016) Decreased expression of hyaluronan synthase 1 and 2 associates with poor prognosis in cutaneous melanoma. *BMC Cancer* **16**, 313.

Preca, B. T., Bajdak, K., Mock, K., Lehmann, W., Sundararajan, V., Bronsert, P., Matzge-Ogi, A., Orian-Rousseau, V., Brabletz, S., Brabletz, T., Maurer, J. and Stemmler, M. P. (2017) A novel ZEB1/HAS2 positive feedback loop promotes EMT in breast cancer. *Oncotarget* **8**, 11530-11543.

Prestwich, G. D. (2011) Hyaluronic acid-based clinical biomaterials derived for cell and molecule delivery in regenerative medicine. *J. Control. Release* **155**, 193-199.

Qin, Z., Dai, L., Bratoeva, M., Slomiany, M. G., Toole, B. P. and Parsons, C. (2011) Cooperative roles for emmprin and LYVE-1 in the regulation of chemoresistance for primary effusion lymphoma. *Leukemia* **25**, 1598-1609.

Ropponen, K., Tammi, M., Parkkinen, J., Eskelinen, M., Tammi, R., Lipponen, P., Agren, U., Alhava, E. and Kosma, V. M. (1998) Tumor cell-associated hyaluronan as an unfavorable prognostic factor in colorectal cancer. *Cancer Res.* **58**, 342-347.

Ryoo, I. G., Choi, B. H., Ku, S. K. and Kwak, M. K. (2018) High CD44 expression mediates p62-associated NFE2L2/NRF2 activation in breast cancer stem cell-like cells: implications for cancer stem cell resistance. *Redox Biol.* **17**, 246-258.

Ryu, D., Lee, J. H. and Kwak, M. K. (2020) NRF2 level is negatively correlated with TGF-β1-induced lung cancer motility and migration via NOX4-ROS signaling. *Arch. Pharm. Res.* **43**, 1297-1310.

Sheng, Y., Cao, M., Liu, Y., He, Y., Zhang, G., Du, Y., Gao, F. and Yang, C. (2021) Hyaluronan synthase 2 (HAS2) regulates cell phenotype and invadopodia formation in luminal-like breast cancer cells. *Mol. Cell. Biochem.* **476**, 3383-3391.

Shibata, T., Ohta, T., Tong, K. I., Kokubu, A., Odogawa, R., Tsuta, K., Asamura, H., Yamamoto, M. and Hirohashi, S. (2008) Cancer related mutations in NRF2 impair its recognition by Keap1-Cul3 E3 ligase and promote malignancy. *Proc. Natl. Acad. Sci. U.S.A.* **105**, 13568-13573.

Son, B., Lee, S., Youn, H., Kim, E., Kim, W. and Youn, B. (2017) The role of tumor microenvironment in therapeutic resistance. *Oncotarget* **8**, 3933-3945.

Sun, Y. (2016) Tumor microenvironment and cancer therapy resistance. *Cancer Lett.* **380**, 205-215.

Takaishi, S., Okumura, T., Tu, S., Wang, S. S., Shibata, W., Vigneshwaran, R., Gordon, S. A., Shimada, Y. and Wang, T. C. (2009) Identification of gastric cancer stem cells using the cell surface marker CD44. *Stem Cells* **27**, 1006-1020.

Tiainen, S., Oikari, S., Tammi, M., Rilla, K., Hämäläinen, K., Tammi, R., Kosma, V. M. and Auvinen, P. (2016) High extent of O-GlcNAcylation in breast cancer cells correlates with the levels of HAS enzymes, accumulation of hyaluronan, and poor outcome. *Breast Cancer Res. Treat.* **160**, 237-247.

Udabage, L., Brownlee, G. R., Nilsson, S. K. and Brown, T. J. (2005) The over-expression of HAS2, Hyal-2 and CD44 is implicated in the invasiveness of breast cancer. *Exp. Cell Res.* **310**, 205-217.

Wang, X. J., Sun, Z., Villeneuve, N. F., Zhang, S., Zhao, F., Li, Y., Chen, W., Yi, X., Zheng, W., Wondrak, G. T., Wong, P. K. and Zhang, D. D. (2008) Nrf2 enhances resistance of cancer cells to chemotherapeutic drugs, the dark side of Nrf2. *Carcinogenesis* **29**, 1235-1243.

Weigel, P. H., Hascall, V. C. and Tammi, M. (1997) Hyaluronan synthases. *J. Biol. Chem.* **272**, 13997-14000.

Yang, C., Sheng, Y., Shi, X., Liu, Y., He, Y., Du, Y., Zhang, G. and Gao, F. (2020) CD44/HA signaling mediates acquired resistance to a PI3Kα inhibitor. *Cell Death Dis* **11**, 831.

Yu, M., Zhang, K., Wang, S., Xue, L., Chen, Z., Feng, N., Ning, C., Wang, L., Li, J., Zhang, B., Yang, C. and Zhang, Z. (2021) Increased SPHK1 and HAS2 expressions correlate to poor prognosis in pancreatic cancer. *Biomed. Res. Int.* **2021**, 8861766.

Yu, Q. and Stamenkovic, I. (1999) Localization of matrix metalloproteinase 9 to the cell surface provides a mechanism for CD44-mediated tumor invasion. *Genes Dev.* **13**, 35-48.